Theoretical Treatment of Diffusional Transport into and through an Oil-Water Emulsion with an Interfacial Barrier at the Oil-Water Interface

TOSHIHISA YOTSUYANAGI, WILLIAM I. HIGUCHI[▲], and ABDEL-HALIM GHANEM

Abstract □ The transport of solute into and through a heterogeneous system involving interfacial barriers was theoretically investigated. The system consisted of a "donor" bulk aqueous phase, the aqueous diffusion layer, and a matrix in which oil droplets of uniform size were dispersed. The theoretical method employed was able to account quantitatively for the barriers existing at the oil droplet-water interface, and the technique should have general applicability to all situations involving a heterogeneous medium in which the local interface equilibrium is achieved slowly. Computations were carried out using the interfacial barrier permeability coefficient, the volume fractions of the phases, and the particle size of the oil droplet as the parameters.

Keyphrases □ Diffusion through oil-water emulsions—theoretical treatment of interfacial barriers, calculation of influence of barrier permeability coefficient, phase volume fraction, and particle size □ Interfacial barriers, oil-water emulsions—theoretical treatment of solute transport rates □ Heterogeneous systems—theoretical treatment of transport rates involving interfacial barriers □ Transport of solutes through heterogeneous system—theoretical treatment of interfacial barriers

When mass transfer occurs into and through polyphase media, especially those involving finely dispersed heterogeneous phases, various factors influence the transport behavior of solutes. Among these factors, the transport resistances existing at the dispersed phase–continuous phase boundaries would be expected to be very important in certain situations (1–3). Yet little is understood about the problem.

The purpose of this study is to describe a procedure for the computations of the transport rate of a solute through a matrix containing a dispersion of oil droplets and for which the solute partitioning rate between the local bulk aqueous and the oil droplet phases might be slow and for which the diffusion through the oil droplets might also be slow (1). The general technique should be applicable to any situation involving a heterogeneous medium in which the local interface equilibrium is achieved slowly. Thus, for example, this approach should also be applicable to the treatment of transport and distribution rate data of drugs in various biological tissues in which the interfacial transport resistance of the cell membrane is appreciable.

THEORY AND GENERAL DESCRIPTION OF MODEL

The system consists of three compartments (Fig. 1). The first compartment is the donor aqueous phase and the second is the aqueous diffusion layer. The third is the matrix in which oil droplets of uniform size are assumed to be dispersed. The donor phase is assumed to be well stirred, and the nature and intensity of the agitation determine the thickness, h, of the diffusion layer. It is assumed that steady-state conditions exist in the diffusion layer, but the distribution of diffusing solute in the matrix compartment follows nonsteady-state diffusion.

In using the finite difference method (4), the matrix compartment is divided into appropriate small segments of equal width. The assumptions on which the model is based are: (*a*) diffusion is one dimensional within the diffusion layer and the matrix, (*b*) the solute begins to penetrate the continuous phase at $t = 0$, (*c*) the number of particles in each segment is constant, and (*d*) the particle size of the oil phase is small compared to the overall dimensions of the transport matrix so that equilibrium inside each oil phase is fast. Then, the solute that enters each segment may be divided into two parts: the portion that goes into the continuous phase and the portion that goes into the oil phase.

The concentration changes with time, t, of the donor phase may be expressed as follows:

$$\frac{dC_b}{dt} = -\frac{D_w A}{V_w h}(C_b - C_{ai}) \qquad \text{(Eq. 1)}$$

where C_b is the concentration of the solute in Compartment I, D_w is the diffusion coefficient of the solute in the diffusion layer, V_w is the volume of Compartment I, A is the surface area exposed, and C_{ai} is the solute concentration at the diffusion layer–matrix interface. The fluxes passing through the interface between the donor phase and the first segment of the matrix are assumed to be equal and may be expressed by:

$$\frac{D_w}{h}(C_b - C_{ai}) = \frac{D_m}{(TH/2)}[C_{ai} - C_{a(1)}] \qquad \text{(Eq. 2)}$$

where D_m is the effective solute diffusion coefficient in the matrix, TH is the thickness of the segment, and $C_{a(1)}$ is the average aqueous solute concentration in the first segment.

The mass balance for each segment is given by:

$$V_t \frac{dC_{t(i)}}{dt} = V_a \frac{dC_{a(i)}}{dt} + V_o \frac{dC_{o(i)}}{dt} \qquad \text{(Eq. 3)}$$

where V_t, V_a, and V_o are the total volume, the volume of the aqueous portion, and the volume of the oil phase, respectively, of a segment;

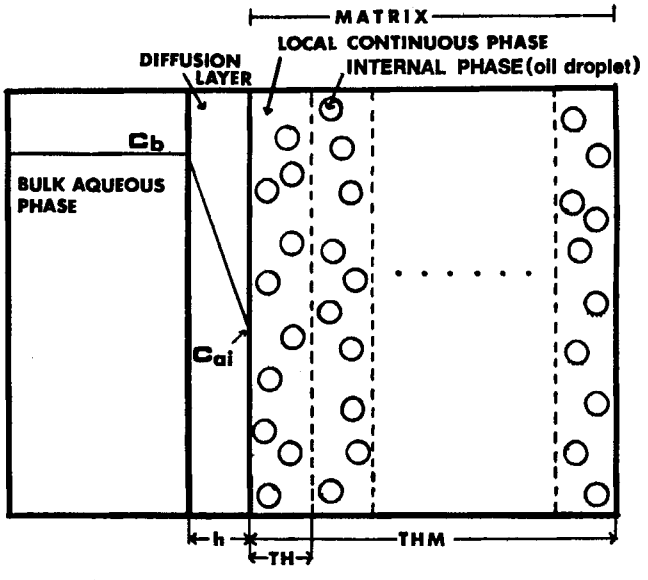

Figure 1—*Schematic model describing the uptake of the solute from the donor bulk aqueous phase to the matrix.* THM *is the thickness of the matrix,* TH *is the thickness of the segment, and* h *is the thickness of the diffusion layer.*

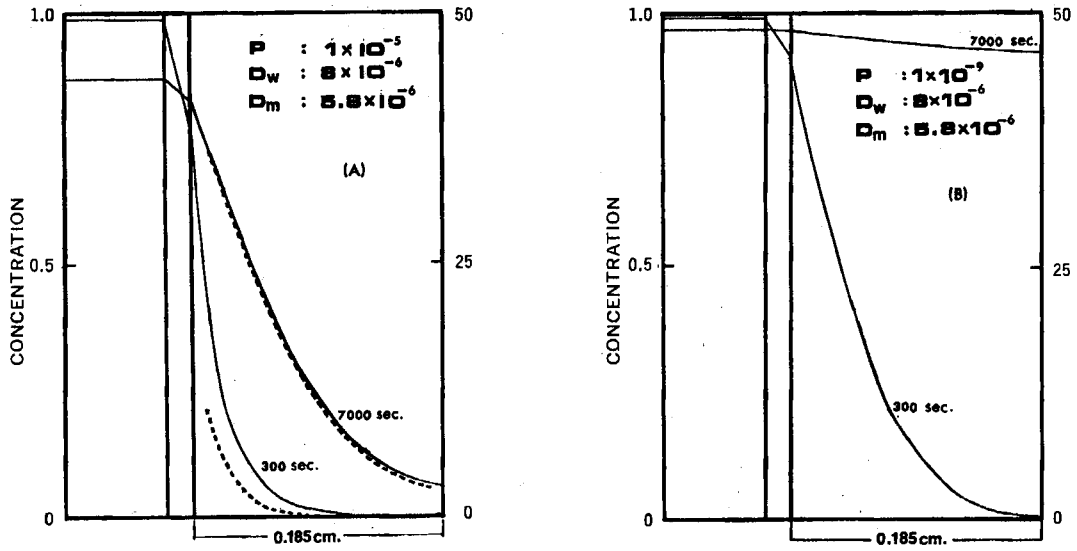

Figure 2—*The concentration–distance distribution profiles in the local bulk aqueous phase (solid line, which corresponds to the left scale) and in the oil phase (dotted line, which corresponds to the right scale). Permeability coefficients are* $P = 1 \times 10^{-5}$ *cm. sec.*$^{-1}$ *(A) and* 1×10^{-9} *cm. sec.*$^{-1}$ *(B). The diffusion coefficient of the donor aqueous phase is* $D_w = 8 \times 10^{-6}$ *cm.*^{2} *sec.*$^{-1}$. *The diffusion coefficient in the matrix is* $D_m = 5.8 \times 10^{-6}$ *cm.*^{2} *sec.*$^{-1}$. *Volume fractions of the aqueous and the oil phases are 0.8 and 0.2, respectively. Other parameters remain fixed.*

$C_{a(i)}$ and $C_{o(i)}$ are the aqueous solute concentration and the oil phase concentration of the solute in segment i, respectively. One may also write the following relations involving the first segment:

$$\frac{dC_{t(1)}}{dt} = \frac{2AD_m}{THV_t}[C_{ai} - C_{a(1)}] - \frac{AD_m}{THV_t}[C_{a(1)} - C_{a(2)}] \quad \text{(Eq. 4)}$$

$$\frac{dC_{o(1)}}{dt} = \frac{n4\pi a^2 P}{V_o}\left[C_{a(1)} - \frac{C_{o(1)}}{K_{ao}}\right] \quad \text{(Eq. 5)}$$

where $C_{a(2)}$ is the aqueous concentration of segment 2, a is the radius of the oil droplet, n is the number of droplets in a segment, P is the permeability coefficient for the oil–water interfacial barrier, and K_{ao} is the oil–water partition coefficient.

The following equations may be written where segment i is neither the first nor the last in the matrix:

$$\frac{dC_{t(i)}}{dt} = \frac{AD_m}{THV_t}[C_{a(i-1)} - 2C_{a(i)} + C_{a(i+1)}] \quad \text{(Eq. 6)}$$

$$\frac{dC_{o(i)}}{dt} = \frac{n4\pi a^2 P}{V_o}\left[C_{a(i)} - \frac{C_{o(i)}}{K_{ao}}\right] \quad \text{(Eq. 7)}$$

The rate expressions for the last segment, segment n, are:

$$\frac{dC_{t(n)}}{dt} = \frac{AD_m}{THV_t}[C_{a(n-1)} - C_{a(n)}] \quad \text{(Eq. 8)}$$

Table I—Parameters Describing the System and Their Numerical Values and Dimensions

Parameter	Values
D_w	8×10^{-6} (cm.^{2} sec.$^{-1}$)
D_m	5.8×10^{-6} (cm.^{2} sec.$^{-1}$)
h	0.085 (cm.)
V_w	50 (cm.^{3})
THM	0.185 (cm.)
P	$0 \rightarrow \infty$ (cm. sec.$^{-1}$)
a	2.3×10^{-4}, 0.5×10^{-4} (cm.)
V_o	0.8, 0.5
V_a	0.2, 0.5
CONCN1[a]	1 (mole)
A	0.37 (cm.)
K_{ao}	50
NOSEG[b]	10

[a] CONCN1 = initial concentration in the donor phase. [b] NOSEG = number of segments divided.

$$\frac{dC_{o(n)}}{dt} = \frac{n4\pi a^2 P}{V_o}\left[C_{a(n)} - \frac{C_{o(n)}}{K_{ao}}\right] \quad \text{(Eq. 9)}$$

Accordingly, the concentrations of drug in the bulk aqueous phase and in each segment in the matrix can be calculated as a function of time by solving the set of differential equations, Eqs. 1–9.

The transport behavior for a typical situation was simulated by the IBM 360/67 digital computer. The parameters selected for the calculations are shown in Table I along with the other input data. The calculations were then carried out for several sets of values of the interfacial barrier permeability coefficient, the volume fraction of the phases, and the oil phase particle size. The detailed outline of the method of computation is given in the *Appendix*.

RESULTS AND DISCUSSION

Typical profiles of the solute concentration–distance distribution in the local bulk aqueous phase and in the oil phase with time are shown in Figs. 2A and 2B. These were simulated under the conditions where the interfacial barrier permeability coefficient, P, was 10^{-5} and 10^{-9} cm. sec.$^{-1}$, respectively. The total penetration into the oil phase is shown in Fig. 3 for three P values. These results show that a strong effect of the permeability coefficient is evident in this range of P values. When the permeability coefficient is 10^{-5}

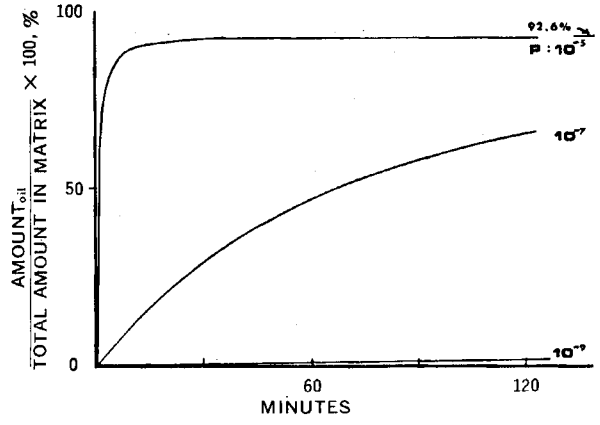

Figure 3—*Time dependence of solute penetration into the total oil phase of the matrix. At equilibrium, the amount in the oil phase is 92.6% of the total amount in the entire matrix.*

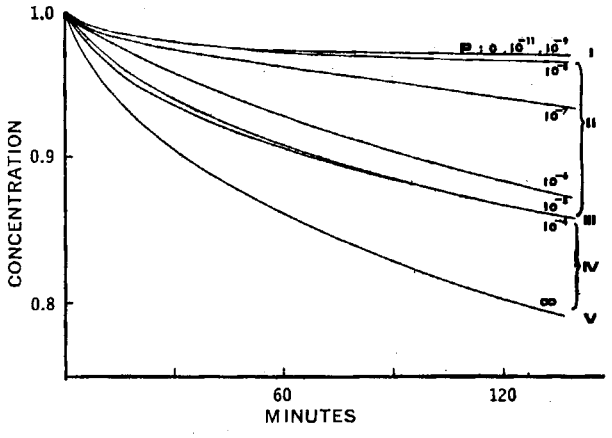

Figure 4—*The concentration change of the donor phase for different oil–water permeability coefficients.* $D_w = 8 \times 10^{-6}$ *cm.*^{2} *sec.*$^{-1}$, $D_m = 5.8 \times 10^{-6}$ *cm.*^{2} *sec.*$^{-1}$, $V_a = 0.8$, $V_o = 0.2$, *and* $a = 2.3 \times 10^{-4}$ *cm. The calculations for* $0 < P \leqq 10^{-4}$ *are carried out with the present procedure. The calculation for* $P = \infty$ *is based upon a previous procedure (5) using the Bruggeman mixture relationship (6) for* D_m.

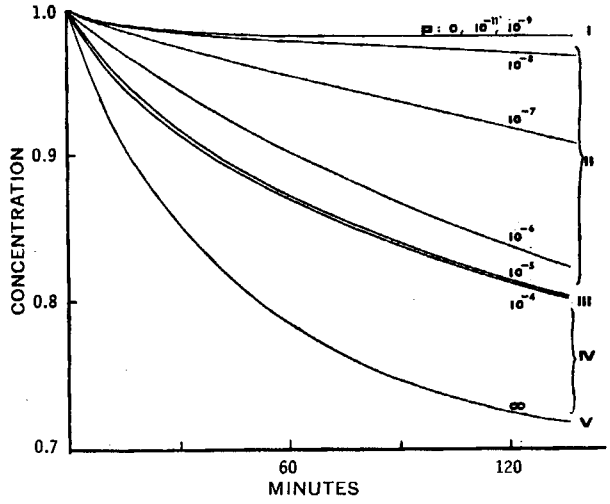

Figure 6—*The solute concentration changes in the donor phase for different permeability coefficients.* $D_w = 8 \times 10^{-6}$ *cm.*^{2} *sec.*$^{-1}$, $D_m = 5.8 \times 10^{-6}$ *cm.*^{2} *sec.*$^{-1}$, $V_a = 0.5$, $V_o = 0.5$, *and* $a = 2.3 \times 10^{-4}$ *cm.*

cm. sec.$^{-1}$, the distribution rate between the local aqueous phase and the oil phase is very fast, and the solute distribution between the aqueous and the oil phases is nearly at equilibrium about 30 min. later. On the other hand, in the case of $P = 10^{-9}$ cm. sec.$^{-1}$, the amount that enters the oil phase is only 2% of the total amount even at $t = 2$ hr. Figure 4 gives the results of the present calculations and those for additional situations expressed in terms of the time changes in the donor phase solute concentration. The only parameter that was varied in these calculations was P from zero to infinity. The other parameters, shown in Table I, remained fixed.

These results may be summarized in the following manner. For the case of extremely low P values, *i.e.*, from zero to 10^{-9} cm. sec.$^{-1}$, the uptake rates for these situations were nearly the same and are classified in the first group. For the range of P values of $10^{-8} \simeq P \simeq 10^{-5}$, the uptake rate was rather sensitive to P and are classified in the second group. The third groups' results correspond to $10^{-5} \simeq P \simeq 10^{-6}$, where again the uptake behavior is somewhat insensitive to P. When the P values are larger than 10^{-4} cm. sec.$^{-1}$ but not very large, the uptake rates again increase with increasing P. This region is classified as the fourth group. When the P is very large, the maximum rate is approached and these results are classified as the fifth group. For this last situation, the present method of calculation was not used. Instead a previous procedure (5) and a D_m value were used based upon the Bruggeman mixture equation (6).

The physical description of these results may be conveniently presented with the help of Fig. 5, in which the effects of changing the permeability coefficient are schematically illustrated. The first situation (Group I results) corresponds to that in which P is so small that oil phase droplets act as impermeable spheres (*e.g.*, glass beads) and only a little solute enters the internal phase. The second situation is that in which the solute distribution rate between the continuous phase and the internal one is still relatively slow but begins to influence significantly the uptake kinetics. For this situation, the partition coefficient, K_{ao}, may not be so influential when it is large and when P is in the lower end of this range. In the third situation (III), the solute distribution is sufficiently fast and the aqueous–oil equilibrium is essentially maintained throughout the matrix. In the fourth situation, the P values are sufficiently great so that the oil droplets are not only locally equilibrated with the aqueous phase but are contributing as significant pathways to the transport of solute. Finally, when P approaches infinity the oil droplets are both fully equilibrated with the aqueous phase and maximally contributing to the effective diffusion coefficient of the heterogeneous system (5).

Figure 6 shows the effect of changing the volume fraction ratio from 0.8/0.2 to 0.5/0.5. As can be seen, there are no significant qualitative differences with the results in Fig. 4. However, the effects are much larger as might be expected.

The effect of particle size is shown in Fig. 7. The particle-size effect is largely restricted to Group II results, where the larger the size of the oil droplets the faster is the uptake rate. However, for much larger and for much smaller P values, the particle size should have no effect on the uptake kinetics.

This study has provided a quantitative method for analyzing the transport behavior of solutes through a heterogeneous system in which local interfacial barriers play important roles in determining: (*a*) the extent to which the internal phase is in equilibrium with the

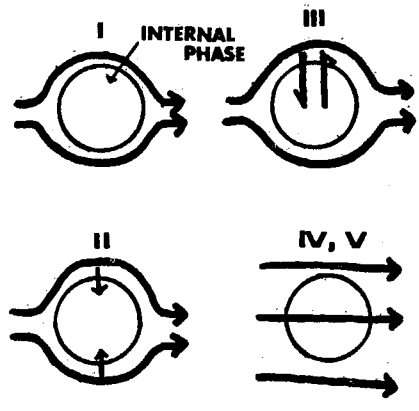

Figure 5—*Schematic illustrations of drug transport through the continuous phase (aqueous bulk phase) and involving the internal phase (oil phase), corresponding to different situations dependent upon the magnitude of the interfacial barrier permeability coefficient.*

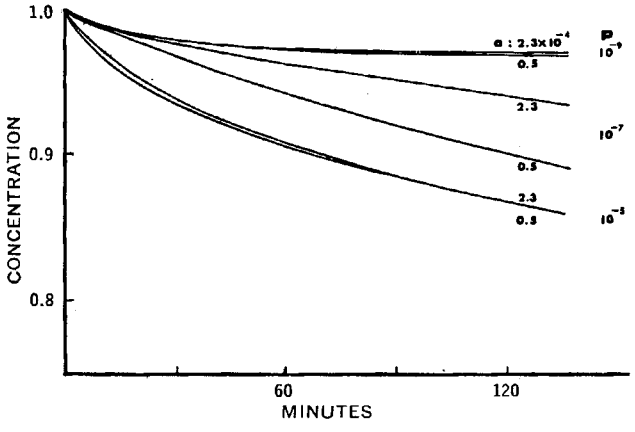

Figure 7—*Effect of particle size on the solute uptake rate. Particle radius* $= 2.3 \times 10^{-6}$ *cm. and* 0.5×10^{-4} *cm.,* $V_a = 0.8$, *and* $V_o = 0.2$.

local continuous phase, and (*b*) the extent to which the internal phase acts as a pathway for transport of the solute. The theoretical procedure permits the calculation of the influences of the interfacial barrier permeability coefficient, the particle size, the volume fractions of the phases, and the partition coefficients in the phases upon the solute transport rates through the heterogeneous media.

APPENDIX: NUMERICAL COMPUTATION PROCEDURE

The flow diagram of the calculating procedure is briefly shown in Scheme I. After $t = 0$, a series of calculation procedures undergo

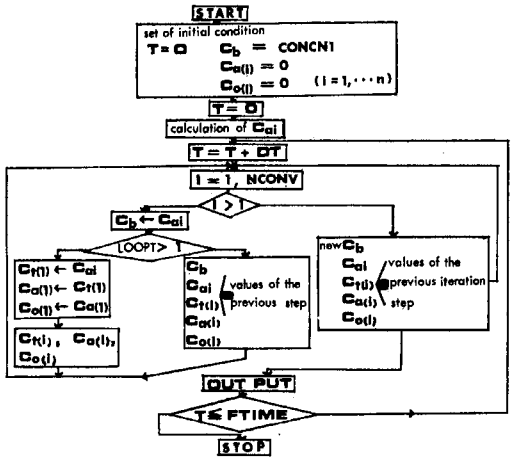

Scheme I—Flow diagram for computation of concentration distributions

successive approximation for each time increment, Δt. On the calculation of C_b, $C_{t(i)}$, $C_{a(i)}$, and then $C_{o(i)}$ at $t = \Delta t$, the first approximation of ΔC_b is obtained from Eq. 1, assuming $(C_{ai})_{t=\Delta t} = (C_{ai})_{t=0}$. Then under the assumption of both $C_{a(i)}$ and $C_{a(i+1)} = 0$, the first approximation of $\Delta C_{t(i)}$ is calculated by Eqs. 4, 6, and 8, respectively, and then $C_{t(i)}$ at $t = \Delta t$ is assumed $\Delta C_{t(i)}$ for $0 < t \leqq \Delta t$. Next, by assuming $\Delta C_{o(i)} = 0$, $\Delta C_{t(i)} = \Delta C_{a(i)}$ according to Eq. 3 and then $C_{a(i)}$ is also assumed $0.5 \times \Delta C_{a(i)}$ for $0 < t \leqq \Delta t$. Accordingly, $\Delta C_{o(i)}$ is calculated by Eqs. 5, 7, and 9, respectively, under the assumption of $C_{o(i)} = 0$, and then $C_{o(i)}$ is assumed $0.5 \times \Delta C_{o(i)}$ for $0 < t \leqq \Delta t$. The second approximations of C_{ai}, C_b, $C_{t(i)}$, $C_{a(i)}$, and $C_{o(i)}$ are calculated by using the first approximations successively. These procedures are repeated until respective values converge. The calculation of the next step (added Δt) starts from the values of one step before in the same manner mentioned above.

REFERENCES

(1) A.-H. Ghanem, W. I. Higuchi, and A. P. Simonelli, *J. Pharm. Sci.*, **59**, 659(1970).

(2) A. B. Bikhazi and W. I. Higuchi, *ibid.*, **59**, 744(1970).

(3) V. Surpuriya and W. I. Higuchi, *ibid.*, **61**, 375(1972).

(4) J. Crank, "Mathematics of Diffusion," Oxford, New York, N. Y., 1956.

(5) S. A. Howard, A. Suzuki, M. A. Farvar, and W. I. Higuchi, *J. Pharm. Sci.*, **58**, 1325(1969).

(6) W. I. Higuchi, *ibid.*, **56**, 315(1967).

ACKNOWLEDGMENTS AND ADDRESSES

Received June 19, 1972, from the *College of Pharmacy, University of Michigan, Ann Arbor, MI 48104*

Accepted for publication August 11, 1972.

▲ To whom inquiries should be directed.

A New Tablet Disintegrating Agent: Cross-Linked Polyvinylpyrrolidone

SAUL S. KORNBLUM▲ and SAMUEL B. STOOPAK

Abstract □ Cross-linked polyvinylpyrrolidone was studied for its disintegration property in comparison to starch USP and alginic acid. Certain physical parameters of the disintegrants (maximum moisture sorption, hydration capacity, bulk density, and specific surface area) were determined for the purpose of differentiating their relative efficiency. A linear relationship was found to exist when the maximum moisture sorption was plotted *versus* the specific surface area for each disintegrant. It was postulated that capillary activity of the cross-linked polyvinylpyrrolidone for water appears responsible for its tablet disintegration property. Cross-linked polyvinylpyrrolidone demonstrated superiority over starch USP and alginic acid in most of the experimental tablet formulations made by either dry or wet granulation. A quinazolinone compound was formulated into tablets employing each disintegrant to provide identical disintegration times, and these tablets were submitted to dissolution rate analysis. The dissolution results showed some differences for those made by direct compression but no variation for wet granulated tablets.

Keyphrases □ Polyvinylpyrrolidone, cross linked—evaluated as tablet disintegrant, compared to starch USP and alginic acid □ Tablet disintegrants—cross-linked polyvinylpyrrolidone evaluated, compared to starch USP and alginic acid □ Disintegration properties—cross-linked polyvinylpyrrolidone, compared to starch USP and alginic acid

Today's emphasis on the availability of drugs highlights the importance of the relatively rapid disintegration of a tablet as a criterion for ensuring uninhibited drug dissolution behavior (1–3). Only a few acceptable tablet disintegrating agents are available to the research pharmacist. The starches (corn, potato, wheat, rice, and arrowroot) have been extensively studied (4–7) as to their varying properties as disintegrants (8). The mechanism of action of the starches is still undergoing study, although at one point it was wrongly felt that grain swelling was responsible (7). Experiments with compressed starch, both dry and wetted, observed with